Quantification and Visualization of the Transport of Octreotide, a Somatostatin Analogue, Across Monolayers of Cerebrovascular Endothelial Cells

Ulrich Jaehde,[1,4] Rosalinde Masereeuw,[1] Albertus G. De Boer,[1,5] Gert Fricker,[3] J. Fred Nagelkerke,[2] J. Vonderscher,[3] and Douwe D. Breimer[1]

Received June 1, 1993; accepted October 9, 1993

Confocal laser scanning microscopy (CLSM) was used to quantify and visualize the transport of the octapeptide and somatostatin analogue, octreotide (SMS 201-995, Sandostatin), across monolayers of bovine cerebrovascular endothelial cells, an *in vitro* model of the blood–brain barrier. The concentrations of octreotide and its conjugates in the cell culture medium were determined by radioimmunoassay (RIA). Two fluorescent conjugates of octreotide (FITC- and NBD-octreotide) were used to obtain CLSM images. The peptides did not undergo significant degradation in the presence of brain endothelial cell monolayers. The transport rate of octreotide expressed as clearance (Cl) and endothelial permeability (P_e) did not depend on either the initial concentration (between 10 n*M* and 1 μ*M*) or the site of administration (luminal or abluminal side of the monolayer), indicating the absence of saturable and/or asymmetrical transport mechanisms. The P_e of octreotide and that of the paracellular permeability marker fluorescein correlated well. Although the conjugates are more lipophilic than octreotide itself, they exhibited lower Cl and P_e, values probably because of their larger molecular size. On the CLSM images, FITC-octreotide was present only in the intercellular space, while the cells did not exhibit detectable fluorescence. Transport studies and CLSM images suggest that octreotide passes the endothelial monolayer primarily via the paracellular route without significant contribution of carrier-mediated transport.

KEY WORDS: octreotide; somatostatin analogue; SMS 201-995; peptides; blood–brain barrier; transport; visualization; confocal laser scanning microscopy.

INTRODUCTION

Several cell culture models have been established for the characterization of drug transport and metabolism *in vitro* (1), but there are still limitations regarding the prediction of *in vivo* permeability (2). Confocal laser scanning microscopy (CLSM) can visualize transport routes of drugs across cell layers *in vitro*. CLSM has advantages over conventional microscopy such as improved resolution and contrast and the removal of out-of-focus light (3). Using CLSM, biological specimens can be optically sectioned to localize fluorescent molecules in living cells without any physical damage to the specimen (3). Recently, this method was applied to visualize the transport of poly-L-lysine and insulin across the cornea (4). In our investigation a cell culture model of the blood–brain barrier was used consisting of primary cultures of isolated bovine cerebrovascular endothelial cells (5,6). Monolayers of those cells have been shown to retain many *in vivo* characteristics of the brain endothelium such as tight junctions and the presence of specific blood–brain barrier enzyme markers (5,6).

The somatostatin analogue octreotide (SMS 201-995, Sandostatin) was chosen for this study. Peptide transport across the blood–brain barrier has been intensively studied (7–9). Octreotide is an octapeptide with activity similar to that of somatostatin, including the suppression of the secretion of growth hormone (10). Compared to somatostatin, octreotide has a considerably longer half-life due to its relatively high metabolic stability (11). Clinical studies have shown its efficacy in the treatment of acromegaly and gastrointestinal neuroendocrine tumors (10). Additional applications have been discussed, particularly in the cancer field (12,13). Since a high density of somatostatin receptors has been reported in several tumors of the CNS (14), octreotide may be of value in the treatment and localization of these tumors.

The aim of this investigation was to characterize the transport kinetics and to visualize the transport routes of octreotide across monolayers of cerebrovascular endothelial cells. Confocal fluorescence images were obtained using two fluorescent conjugates of octreotide: fluorescein isothiocyanate (FITC)-octreotide and 4-nitrobenzo-2-oxa-1,3-diazol (NBD)-octreotide. The latter was recently used to visualize the enteral absorption of octreotide (15). Since fluorescence derivatization alters lipophilicity and molecular size, the transport characteristics of the conjugates were studied in comparison to octreotide itself. All compounds were examined for metabolic stability in the presence of cerebrovascular endothelial cells.

MATERIALS AND METHODS

Materials

Octreotide (SMS 201-995) and the conjugates FITC-octreotide and NBD-octreotide were synthesised by the Preclinical Research Department, Sandoz Pharma Ltd., Basel, Switzerland.

Determination of the Apparent Partition Coefficient

Each compound was dissolved at a concentration of 1 μ*M* in *n*-octanol-saturated 0.1 *M* phosphate buffer, pH 7.4. Two milliliters of each solution was added to an identical volume of *n*-octanol (Fluka AG, Buchs, Switzerland). The

[1] Division of Pharmacology, Leiden/Amsterdam Center for Drug Research, Leiden University, P.O. Box 9503, 2300 RA Leiden, The Netherlands.
[2] Division of Toxicology, Leiden/Amsterdam Center for Drug Research, Leiden University, P.O. Box 9503, 2300 RA Leiden, The Netherlands.
[3] Drug Delivery Systems, Sandoz Pharma Ltd., Basel, Switzerland.
[4] Current address: Institute of Pharmacy, Free University of Berlin, Kelchstr. 31, D-12169 Berlin, Germany.
[5] To whom correspondence should be addressed.

0724-8741/94/0300-0442$07.00/0

mixture was continuously shaken for 30 min and subsequently centrifuged for 10 min. Concentrations in the aqueous phase before and after the octanol/buffer partition were assayed by radioimmunoassay (RIA). The apparent partition coefficient (P) at pH 7.4 was calculated dividing the concentration in the octanol phase by that in the aqueous phase. Each determination was performed in triplicate.

Cell Isolation and Culture

The procedure of Audus and Borchardt (5) was modified to isolate cerebrovascular endothelial cells from freshly obtained bovine brains as described previously (6). For initiation of the cell cultures, Transwell-Col filters (Costar Corp., Cambridge, MA) with a surface area of either 4.71 cm^2 for the transport experiments or 0.33 cm^2 for confocal laser scanning microscopy were placed on a plate with 6 or 24 wells, respectively. For the metabolism experiments, plastic wells with a surface area of 1.6 cm^2 were used. Filters and wells were coated with rattail collagen and fibronectin. The endothelial cells were seeded at a density of 400,000 to 500,000 cells per cm^2. Cell culture medium (CCM) (6) was added to both sides of the filter or to the well, respectively. The cells were cultured at 37°C under an atmosphere of 95% oxygen and 5% carbon dioxide until a confluent monolayer was obtained after 8 days. The confluent monolayers were used for the experiments. The cells were characterized by electron microscopy, Ac-LDL uptake, and γ-glutamyl transpeptidase activity (H. E. de Vries, personal communication).

Transport Experiments

The endothelial permeability was determined by means of transport experiments in CCM at 37°C.

Three hours before the experiment, the confluency of each monolayer was confirmed by phase-contrast microscopy. As a control of the quality of each monolayer, the transendothelial electrical resistance (TEER) was measured about 90 min before the experiment using two sets of Ag/AgCl electrodes. One set of electrodes was placed above, and the other set was placed underneath monolayer and filter. A 10-V, 10-Hz block pulse was generated by a PM 5131 function generator (Philips, Eindhoven, The Netherlands). The difference in potential was amplified by a Model 113 differential amplifier (Princeton Applied Research PAR, Princeton, NJ). The TEER was calculated according to

$$\text{TEER} = (R_t - R_f) \cdot A \quad (1)$$

R_t is the total resistance of the filter and monolayer, R_f is the resistance of the filter only, and A is the surface area of the monolayer (4.71 cm^2).

Subsequently, the medium was changed, and after a 3-hr incubation period, the transport experiment was started by adding a solution of the test compound in CCM to either the luminal or the abluminal side of the monolayer to have an initial concentration of either 10 nM or 1 μM. Simultaneously, 1 μg/mL of fluorescein sodium (Sigma Chemical Co., St. Louis, MO) was administered as a permeability marker. At 15, 30, 45, 60, 75, and 90 minutes after the onset of the experiment, two 100-μL samples were taken from the acceptor side for RIA and fluorescence analysis and replaced with 200 μL of prewarmed CCM. The concentrations in the acceptor chamber were corrected for sampling. In addition, two 50-μL samples from the donor side were taken immediately and 90 min after addition of the test compound. At the end of the transport experiment, the endothelial monolayer was microscopically examined upon integrity. Control experiments without monolayer were performed under identical conditions to determine the permeability of the filter to each individual compound.

Metabolism Experiments

The metabolism of octreotide and its conjugates in the presence of cerebrovascular endothelial cells was studied by incubating a 1 μM solution of octreotide and its analogues in CCM for 24 hr with a monolayer of endothelial cells grown on a collagen/fibronectin-coated plastic well at 37°C. At 1, 2, 4, 6, and 24 hr after onset of the experiment, 50-μL samples were taken and analyzed by RIA. A control experiment without cells was performed under identical conditions.

Drug Analysis

The concentrations of octreotide and its conjugates in cell culture medium were determined by a RIA using rabbit antiserum and ^{125}I-labeled octreotide as a tracer (16). The antiserum was found to be specific for intact octreotide, whereas fragments bound only to a negligible extent. Sac-Cel anti-rabbit serum (Wellcome Diagnostics, Utrecht, The Netherlands) was used for the separation of free and bound peptide. The calibration curves of the conjugates were parallel to that of octreotide (Fig. 1). Each determination was performed in duplicate. The detection limit of the assay was about 10 pg/mL for octreotide, 50 pg/mL for FITC-octreotide, and 100 pg/mL for NBD-octreotide. Cross-reactivity was found to be 14.6% for FITC-octreotide and 8.2% for NBD-octreotide. The between-day precision of the assay was found to be 9.6% using a concentration of 100 pg/mL octreotide in cell culture medium.

Data Analysis

The amount of drug transported across the endothelial

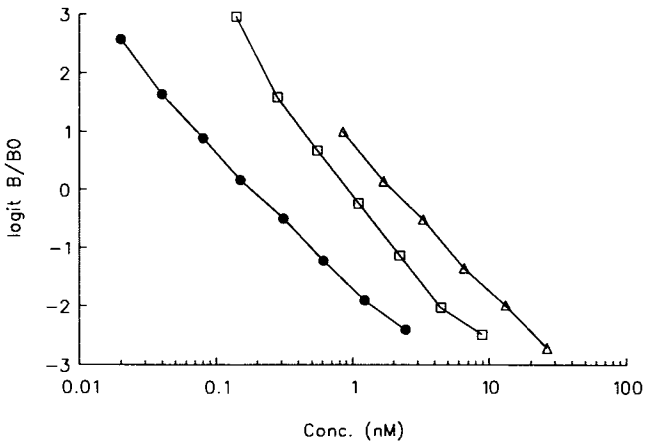

Fig. 1. Mean RIA calibration curve of octreotide (●; n = 11), FITC-octreotide (□; n = 3), and NBD-octreotide (△; n = 2).

monolayer and filter was expressed as the cumulative cleared volume of the donor chamber. The slope of the cumulative cleared volume versus time curve (clearance Cl) was used to calculate the permeability P:

$$P = Cl/A \quad (2)$$

The endothelial permeability P_e was calculated from the experimentally determined individual total permeability of cells and filter (P_t) and the average permeability of the filter alone (P_f) (6):

$$1/P_e = (1/P_t) - (1/P_f) \quad (3)$$

The endothelial permeability of the marker compound fluorescein sodium (P_m) was used to characterize the basal paracellular permeability of individual monolayers (1,17), which may differ among different batches of isolated endothelial cells. P_e was related to P_m by calculating the transport index (TI) (17):

$$TI = P_e \cdot 100/P_m \quad (4)$$

The one-way analysis of variance (ANOVA) was used to detect significant differences. The significance level was set to $P < 0.05$. The homogeneity of variance was assessed by Bartlett's test. Linear regression analysis was performed to describe the relationship between the permeability of octreotide and the marker compound fluorescein.

Confocal Laser Scanning Microscopy

The endothelial cell monolayers were incubated with the fluorescent octreotide conjugates for 30 to 60 min either at 37°C or at room temperature. Subsequently, the medium was removed and the filters were placed directly on a glass coverslip with a thickness of 0.13 to 0.15 mm.

Confocal fluorescent images were obtained with a MRC-600 (Bio-Rad Microscience Ltd., Hemel Hempstead, England) confocal laser scanning microscope. The laser intensity was reduced by a neutral density filter to 1% to minimize photobleaching. The microscope was equipped with a Zeiss 63× Planapo oil immersion objective exhibiting a numerical aperture of 1.4. Optical horizontal (XY) and perpendicular (XZ) sections were recorded and printed using a Video Graphic Printer UP-850 (Sony, Japan).

RESULTS

Lipophilicity

The octanol/buffer partition coefficient (log$P$) at pH 7.4 was determined to assess the effect of fluoresence derivatization on the lipophilic properties of the octreotide molecule. The conjugates were found to exhibit a higher lipophilicity than octreotide (log$P$: -0.16 ± 0.05). NBD conjugation affected lipophilicity more (log$P$: 1.13 ± 0.09) than FITC conjugation (log$P$: 0.37 ± 0.07).

Metabolic Stability

Incubation of 1 μM octreotide and its conjugates in cell culture medium at 37°C with and without monolayer of endothelial cells did not lead to major changes in concentration (Table I). Although the measured concentrations were partly below 100%, we observed neither a time-dependent decline nor any differences between control and monolayer experiments. This suggests that octreotide and its conjugates do not undergo significant metabolic degradation under the experimental conditions used in this study.

Transport Kinetics

The transport parameters of octreotide and its conjugates are summarized in Table II together with the permeability of the marker compound fluorescein (P_m) and the TEER characterizing the monolayers used. The transport profiles of octreotide and its conjugates are shown in Fig. 2.

The batches of cell monolayers used for the octreotide experiments at 10 nM and 1 μM were found to differ from each other in paracellular permeability as indicated by differences in P_m and TEER. For that reason, the TI relating the permeability of octreotide (P_e) to that of the reference compound fluorescein (P_m) was used for statistical analysis. P_e was in all experiments lower than P_m. TI did not differ significantly between the experiments; neither between different initial concentrations nor between luminal and abluminal administration. This suggests that saturable or asymmetrical transport systems do not contribute significantly to the transport of octreotide across the cell monolayer in the concentration range studied. Consequently, we found that the octreotide permeability correlated significantly with that of fluorescein, independent on the initial concentration or the administration site (Fig. 3).

In contrast, the conjugation of octreotide to FITC or NBD altered its transport rate across the monolayer (Fig. 2, Table II). Because of the analytical interference, fluorescein could not be coadministered in the transport studies with the conjugates. The TEER values, however, indicate that the permeability of the monolayers used for all 1 μM experiments did not exhibit major differences. Therefore, P_e was

Table I. Stability (% of the Initial Concentration) of 1 μM Octreotide and Its FITC- and NBD-Conjugate in Cell Culture Medium at 37°C in the Absence and Presence of a Monolayer of Bovine Brain Endothelial Cells (Mean ± SD; $n = 3$)

	Octreotide		FITC-octreotide		NBD-octreotide	
Time (hr)	Without cells	With cells	Without cells	With cells	Without cells	With cells
1	99 ± 3	99 ± 8	81 ± 9	78 ± 7	92 ± 8	89 ± 19
2	93 ± 10	95 ± 10	88 ± 18	103 ± 8	93 ± 9	80 ± 11
4	92 ± 13	108 ± 11	102 ± 5	102 ± 5	93 ± 14	97 ± 23
6	102 ± 10	106 ± 5	87 ± 5	87 ± 7	90 ± 1	85 ± 8
24	105 ± 8	113 ± 8	84 ± 2	89 ± 14	99 ± 4	94 ± 17

Table II. Blood–Brain Barrier Transport Parameters (Cl_f, Cl_t, P_e, TI) of Octreotide and Its FITC- and NBD-Conjugates and Characterization of the Monolayers Used (P_m, TEER) as Mean ± SD (n = 3)[a]

Compound	Site	Conc.	Analysis	Cl_f (μL/min)	Cl_t (μL/min)	P_e (10^{-3} cm/min)	P_m (10^{-3} cm/min)	TI (%)	TEER ($\Omega \cdot cm^2$)
Octreotide	lum	10 n*M*	RIA	10.8 ± 1.0	3.9 ± 0.8	1.30 ± 0.40	1.81 ± 0.54	72 ± 7	13 ± 3
Octreotide	abl	10 n*M*	RIA	9.0 ± 0.6	3.3 ± 0.7	1.12 ± 0.37	1.51 ± 0.38	74 ± 6	14 ± 2
Octreotide	lum	1 μ*M*	RIA	n.d.[b]	2.2 ± 0.4	0.58 ± 0.13	0.89 ± 0.32	67 ± 9	23 ± 1
Octreotide	abl	1 μ*M*	RIA	n.d.[b]	2.0 ± 0.2	0.53 ± 0.09	0.75 ± 0.02	71 ± 9	23 ± 4
FITC-octreotide	lum	1 μ*M*	RIA	6.8 ± 0.4	1.2 ± 0.1	0.31 ± 0.01	n.d.	n.d.	24 ± 4
			Fl	7.0 ± 1.3	1.1 ± 0.1	0.27 ± 0.03			
NBD-octreotide	lum	1 μ*M*	RIA	5.2 ± 0.3	1.4 ± 0.3	0.41 ± 0.11	n.d.	n.d.	22 ± 2

[a] Cl_f, clearance across the filter alone; Cl_t, clearance across filter and monolayer; P_e, endothelial permeability; P_m, endothelial permeability of the marker compound fluorescein; TEER, transendothelial electrical resistance; TI, transport index; lum, luminal administration; abl, abluminal administration; Fl, fluorescence analysis; n.d., not determined.
[b] Cl_f at 10 n*M* was used for calculation of P_e.

used for statistical analysis without further correction. Octreotide was found to have the highest P_e after luminal administration of 1 μ*M* followed by NBD-octreotide and FITC-octreotide. One-way analysis of variance resulted in significant differences between the compounds ($P < 0.05$). The concentrations of FITC-octreotide were determined also by fluorescence measurement. Table II shows that the results obtained by fluorescence analysis were almost identical to the results obtained by RIA.

Visualization of Transport

Confocal laser scanning microscopic images were taken after incubation of confluent monolayers with fluorescein, FITC-octreotide, and NBD-octreotide.

Fluorescein was used to assess whether the experimental setup is suitable to visualize paracellular transport. Figure 4 shows two representative images obtained by horizontal (*XY* plane; Fig. 4A) and vertical (*XZ* plane; Fig. 4B) optical sectioning through the monolayer following a 60-min incubation at 37°C with fluorescein. We found that no fluorescein was present in the intracellular space. The *XY* section (Fig. 4A) showed the spindle-shaped morphology of the endothelial cells. On the *XZ* image (Fig. 4B), the endothelial cells appeared as dark structures between the surrounding medium that contained fluorescein and the fluorescent filter membrane. Since the filter membrane did not show any autofluorescence in control experiments without administration of fluorescent agents, it is suggested that its high fluorescence intensity is due to adsorption or binding of fluorescein to the filter membrane.

FITC-octreotide was found to give comparable images as fluorescein (Fig. 5) following a 37°C incubation. On the *XY* (Fig. 5A) and the *XZ* image (Fig. 5B), FITC-octreotide is visible in the intercellular space and in the surrounding medium. The cells do not exhibit detectable fluorescence. The highest fluorescence intensity was found at the filter membrane. With the NBD conjugate, a comparable image could not be obtained due to its lower fluorescence intensity. Even with a concentration of 200 μ*M* NBD-octreotide, the fluorescence in the surrounding medium was too weak to give a clear contrast between the intra- and the extracellular space. Higher concentrations could not be used because of solubility problems.

After incubation at room temperature, some cells (about 10%) displayed fluorescent dots in the cytoplasma (Fig. 6). We observed this phenomenon with both labels (FITC, Fig.

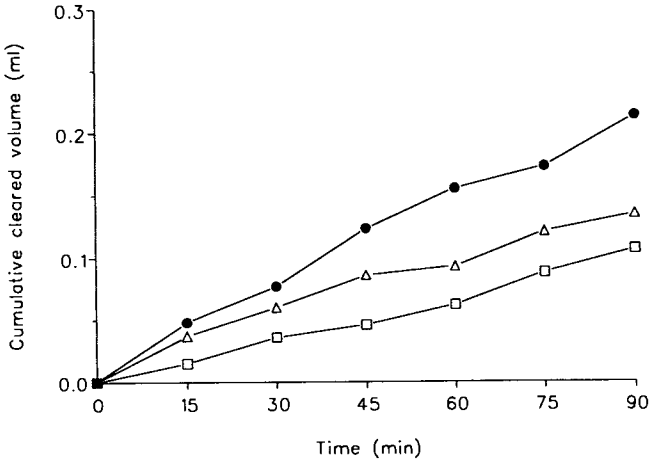

Fig. 2. Mean transport profiles of equimolar concentrations (1 μ*M*) of octreotide (●), FITC-octreotide (□), and NBD-octreotide (△) across cerebrovascular endothelial monolayer and filter shown as the cumulative cleared volume versus time (n = 3).

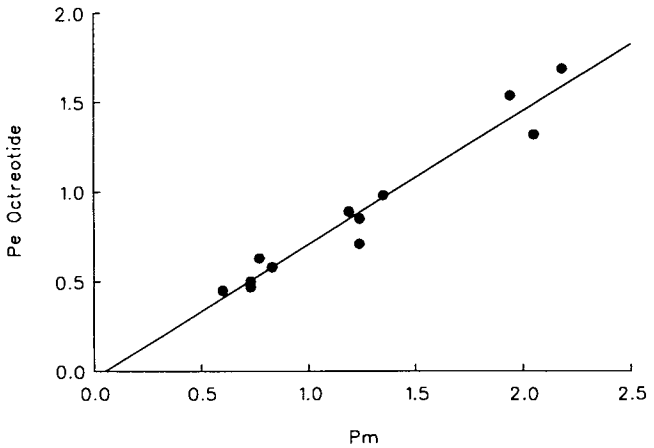

Fig. 3. Relationship between the endothelial permeability of octreotide (P_e) and that of fluorescein (P_m): r = 0.974, $P < 0.001$.

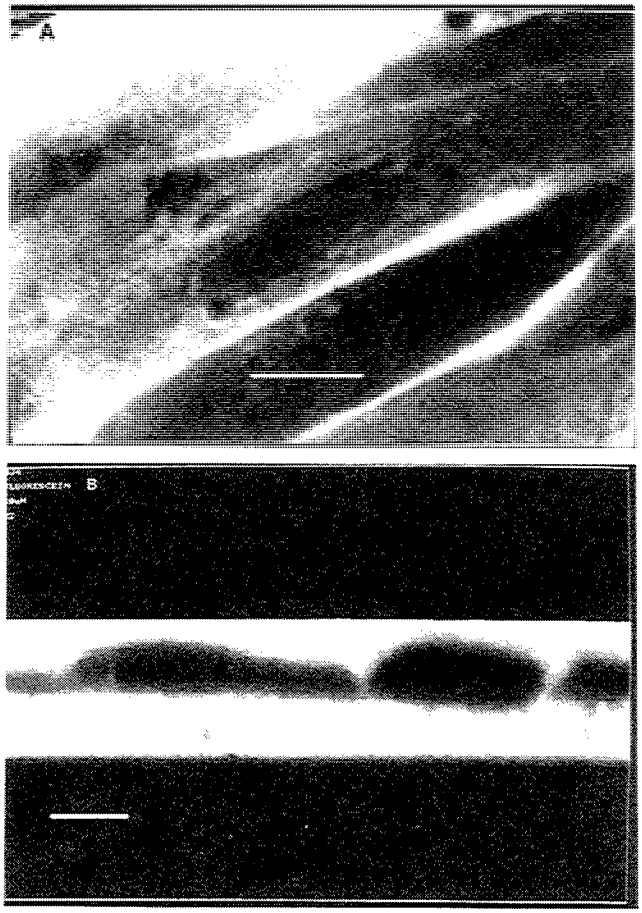

Fig. 4. Confocal laser scanning microscopy images after a 60-min incubation with 10 μ*M* fluorescein at 37°C as *XY* (A) and *XZ* (B) sections. The scale bar represents 10 μm.

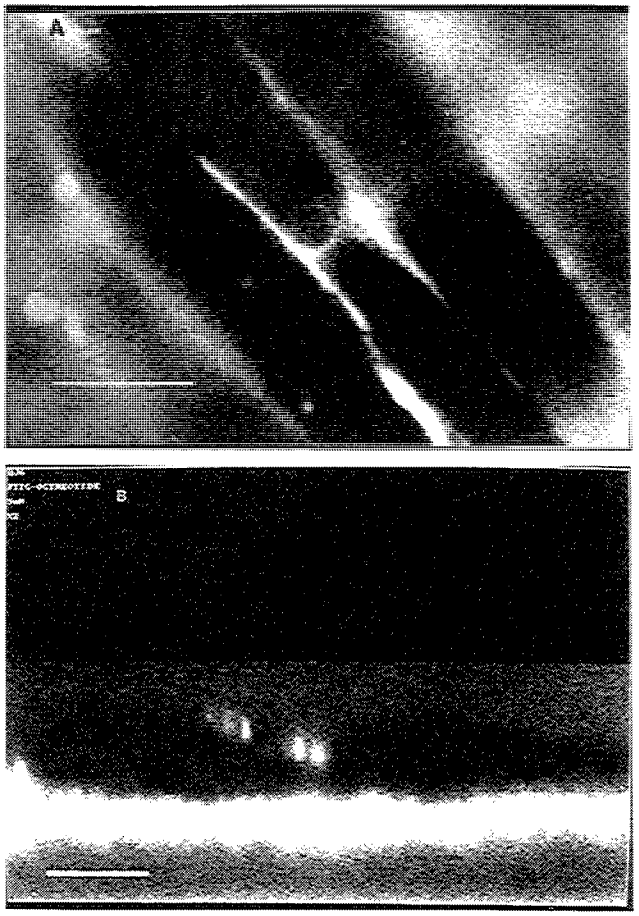

Fig. 5. Confocal laser scanning microscopy images after a 60-min incubation with 5 μ*M* FITC-octreotide at 37°C as *XY* (A) and *XZ* (B) sections. The scale bar represents 10 μm.

6A; NBD, Fig. 6B), even when the concentration in the surrounding medium was too low to give detectable fluorescence. This suggests a punctate accumulation of the conjugates with a local concentration that is considerably higher than the concentration in the surrounding medium.

DISCUSSION

The transport of octreotide across cerebrovascular endothelial cell monolayers *in vitro* was quantified in relation to that of the permeability marker fluorescein and visualized using fluorescent conjugates and confocal laser scanning microscopy. The transport experiments did not reveal any differences in octreotide permeability among different concentrations and/or administration sites. In the setup used the octreotide permeability was strongly correlated with that of fluorescein, suggesting that octreotide passes the monolayer primarily via the paracellular route without any significant transcellular diffusion or carrier-mediated transport involved. The lower permeability value of octreotide (67 to 74%) compared to fluorescein is probably due to the larger molecular weight of the octapepide (1019) compared to that of fluorescein (332) and/or to differences in charge. Unlike octreotide, a saturable transport system in the brain-to-blood direction was reported for two other octapeptide somatostatin analogues in mice (18). The symmetric transport of octreotide which differs from those analogues in two or three amino acids may indicate the high specificity of this carrier or may be attributed to the different techniques used.

The conjugation of octreotide to FITC or NBD caused a decrease in permeability. Since the lipophilicity of the conjugates is considerably higher, this result indicates that molecular size is the major factor governing the permeability of octreotide and its conjugates. Comparing the three compounds, permeability decreases with increasing molecular weight: octreotide (1019) > NBD-octreotide (1183) > FITC-octreotide (1408). This finding supports the idea that octreotide and its conjugates pass the monolayer by size-dependent paracellular diffusion rather than by lipophilicity-dependent transcellular diffusion.

The transport of FITC-octreotide across the endothelial cell monolayer was visualized by confocal laser scanning microscopy. After incubation at 37°C, the FITC conjugate of octreotide was localized between the spindle-shaped endothelial cells, indicating paracellular transport of FITC-octreotide. The results of the transport experiments (concentration independence, correlation between octreotide and fluorescein permeability) are in good agreement with this finding. After incubation at room temperature, fluorescent dots were observed in individual cells, but the reason

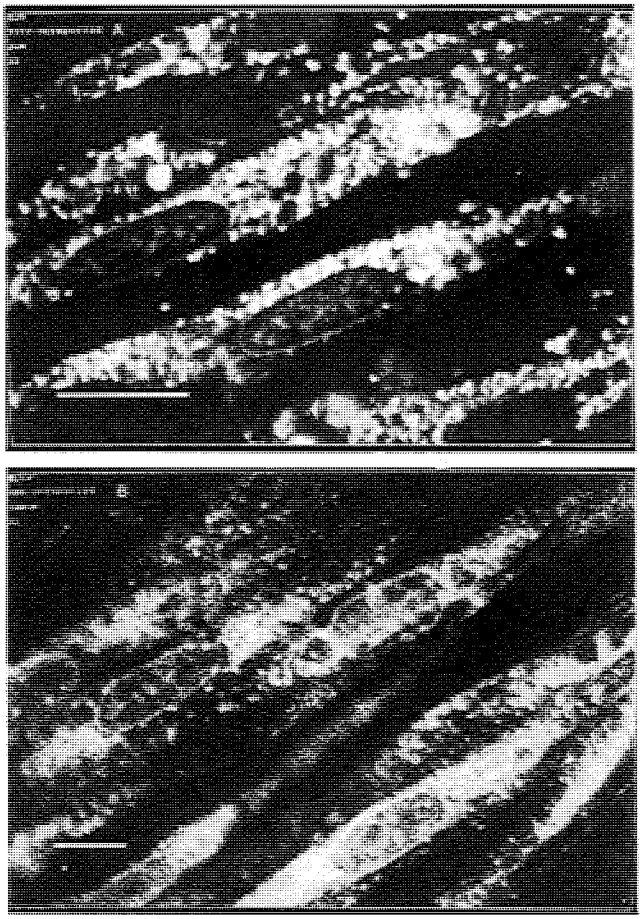

Fig. 6. Confocal laser scanning microscopy images after a 30-min incubation with 2 μM FITC-octreotide (A) and 100 μM NBD-octreotide (B) at room temperature as *XY* sections. The scale bar represents 10 μm.

for this observation is presently unclear. The use of fluorescent labels is often associated with alterations in the physicochemical properties of the compound, such as molecular size and lipophilicity. Indeed, the transport kinetics of octreotide were affected by fluorescence conjugation. Due to limitations in sensitivity, only FITC-octreotide gave a sufficient contrast between high- and low-fluorescent areas.

In the presence of cerebrovascular endothelial cells octreotide was not degraded. Furthermore, we did not find any significant degradation or deconjugation of the FITC and the NBD conjugates under our experimental conditions. The decrease in conjugate concentrations shortly after administration was also observed in the control experiment without any cells. The most likely explanation for this result is adsorption of the conjugates to the plastic wall and/or to the filter membrane. The latter is supported by the confocal microscopic images that show a high fluorescence at the filter membrane following incubation with both labels. Deconjugation of FITC- and NBD-octreotide can be ruled out, since the presence of unlabeled octreotide would have caused an apparent increase in concentration because of its higher affinity to the RIA antiserum (see Fig. 1).

Although our results define the main paracellular transport route of octreotide across the monolayer, the data cannot be used to predict blood–brain barrier permeability *in vivo*. The TEER values of our monolayers (13–24 $\Omega \cdot cm^2$) are much lower than those reported *in vivo* (about 2000 $\Omega \cdot cm^2$) (19), reflecting incomplete formation of tight junctions in culture. *In vitro* systems exhibit higher "leakiness" and hence overestimate paracellular permeability *in vivo* (1,2). Therefore, our results do not prove that octreotide undergoes paracellular transport at the blood–brain barrier *in vivo*. Culture conditions need to be modified to approximate the *in vivo* situation, e.g., by using astrocyte cocultures (20).

ACKNOWLEDGMENTS

This investigation was supported by a grant from Sandoz Pharma Ltd., Basel, Switzerland. The authors gratefully acknowledge the excellent technical assistance of Mrs. M. C. M. Blom-Roosemalen.

REFERENCES

1. K. L. Audus, R. L. Bartel, I. J. Hidalgo, and R. T. Borchardt. The use of cultured epithelial and endothelial cells for drug transport and metabolism studies. *Pharm. Res.* 7:435–451 (1990).
2. W. M. Pardridge, D. Triguero, J. Yang, and P. A. Cancilla. Comparison of in vitro and in vivo models of drug transcytosis through the blood-brain barrier. *J. Pharmacol. Exp. Ther.* 253:884–891 (1990).
3. D. M. Shotton. Confocal scanning optical microscopy and its applications for biological specimens. *J. Cell Sci.* 94:175–206 (1989).
4. Y. Rojanasakul, S. W. Paddock, and J. R. Robinson. Confocal laser scanning microscopic examination of transport pathways and barriers of some peptides across the cornea. *Int. J. Pharm.* 61:163–172 (1990).
5. K. L. Audus and R. T. Borchardt. Characterization of an in vitro blood-brain barrier model system for studying drug transport and metabolism. *Pharm. Res.* 3:81–87 (1986).
6. J. B. M. M. van Bree, A. G. de Boer, M. Danhof, L. A. Ginsel, and D. D. Breimer. Characterization of an in vitro blood-brain barrier: Effects of molecular size and lipophilicity on cerebrovascular endothelial transport rates of drugs. *J. Pharmacol. Exp. Ther.* 247:1233–1239 (1988).
7. W. M. Pardridge. *Peptide Drug Delivery to the Brain,* Raven Press, New York, 1991.
8. J. B. M. M. van Bree, A. G. de Boer, J. Verhoef, M. Danhof, and D. D. Breimer. Peptide transport across the blood-brain barrier. *J. Control. Release* 13:175–184 (1990).
9. W. A. Banks, A. J. Kastin, and C. M. Barrera. Delivering peptides to the central nervous system: Dilemmas and strategies. *Pharm. Res.* 8:1345–1350 (1991).
10. P. E. Battershill and S. P. Clissold. Octreotide. A review of its pharmacodynamic and pharmacokinetic properties, and therapeutic potential in conditions associated with excessive peptide secretion. *Drugs* 38:658–702 (1989).
11. M. Lemaire, M. Azria, R. Dannecker, P. Marbach, A. Schweitzer, and G. Maurer. Disposition of sandostatin, a new synthetic somatostatin analogue, in rats. *Drug Metab. Dispos.* 17:699–703 (1989).
12. A. G. Harris. Future medical prospects for sandostatin. *Metabolism* 39(Suppl. 2):180–185 (1990).
13. B. M. Evers, D. Parekh, C. M. Townsend, and J. C. Thompson. Somatostatin and analogues in the treatment of cancer. *Ann. Surg.* 213:190–198 (1991).
14. J. C. Reubi, W. Lang, R. Maurer, J. W. Koper, and S. W. J. Lamberts. Distribution and biochemical characterization of somatostatin receptors in tumors of the human central nervous system. *Cancer Res.* 47:4758–5764 (1987).
15. G. Fricker, C. Bruns, J. Munzer, U. Briner, R. Albert, T. Kissel, and J. Vonderscher. Intestinal absorption of the octapeptide

SMS 201-995 visualized by fluorescence derivatization. *Gastroenterology* **100**:1544–1552 (1991).
16. W. Bauer, U. Briner, W. Doepfner, R. Haller, R. Huguenin, P. Marbach, T. J. Petcher, and J. Pless. SMS 201-995: A very potent and selective octapeptide analogue of somatostatin with prolonged action. *Life Sci.* 31:1133–1140 (1982).
17. J. N. Cogburn, M. G. Donovan, and C. S. Schasteen. A Model of human small intestinal absorptive cells. 1. Transport barrier. *Pharm. Res.* 8:210–216 (1991).
18. W. A. Banks, A. V. Schally, C. M. Barrera, M. B. Fasold, D. A. Durham, V. J. Csernus, K. Groot, and A. J. Kastin. Permeability of the murine blood-brain barrier to some octapeptide analogs of somatostatin. *Proc. Natl. Acad. Sci. USA* 87:6762–6766 (1990).
19. M. W. Bradbury. Transport across the blood-brain barrier. In E. A. Neuwelt (ed.), *Implications of the Blood-Brain Barrier and Its Manipulation, Vol. 1. Basic Science Aspects*, Plenum Medical Book, New York, 1989, pp. 119–136.
20. M. P. Dehouck, S. Méresse, P. Delorme, J. C. Fruchart, and R. Cecchelli. An easier, reproducible, and mass production method to study the blood-brain barrier in vitro. *J. Neurochem.* 54:1798–1801 (1990).